Ore Geology Reviews 92 (2018) 19–28

Contents lists available at ScienceDirect

Ore Geology Reviews

journal homepage: www.elsevier.com/locate/oregeorev

Surface alteration of a melilitite-clan carbonatite and the potential for remote carbonatite detection

Ethan J. Shavers[a,b], Abduwasit Ghulam[a,b,*], John Encarnacion[b]

[a] Center for Sustainability, Saint Louis University, 3694 West Pine Mall, Saint Louis, MO 63108, USA
[b] Department of Earth and Atmospheric Sciences, Saint Louis University, 3642 Lindell Blvd, Saint Louis, MO, 63108, USA

ARTICLE INFO

Keywords:
Carbonatite
Alnöite
Olivine melilitite
Weathering
Reflectance
Missouri

ABSTRACT

The varied lithologic facies and mineralogy resulting from emplacement of syngenetic alkaline, ultramafic and carbonatite (AUC) intrusions are made more diverse by variable weathering and alteration. Ultramafic-carbonatite intrusive complexes are a source for many valuable minerals including diamonds and rare earth element minerals. The intrusive bodies are often difficult to detect in the field due to their paucity, weathering, vegetation, and, in some instances, similarity to country rock, especially in the case of carbonatites among sedimentary carbonates. Remote spectroscopic detection is used extensively for geologic mapping yet has not been applied to differentiating sedimentary and igneous carbonate weathering profiles. Here we document the alteration mineralogy of a newly authenticated melilitite-clan carbonatite occurrence in the Avon Volcanic District in southeast Missouri, USA. The presence of lizardite, vermiculite, phlogopite, and andradite in the weathered crust of calcic and dolomitic carbonatites differentiate them from sedimentary dolomites. We apply field and laboratory spectral measurements to determine the feasibility of humid region AUC remote sensing and classification. Automated humid region detection and classification of carbonatites among sedimentary carbonates is shown to be possible using ratios of absorption features in the 2000–2400 nm range as well as features centered near 680, 900, and 1100 nm due transition metal charge transfer and crystal field splitting in garnet, sheet-silicates, and spinel.

1. Introduction

Alkaline, ultramafic, and carbonatite (AUC) intrusive complexes are associated with platinum group element, diamond, and rare earth element (REE) deposits (Jones et al., 2013; Mitchell, 2008). In addition, AUC dikes and pipes offer unique insight into Earth's interior. The rapid rate of ascent by AUCs carries up mantle material that is otherwise inaccessible and reveals a great deal about Earth's interior (Giuliani et al., 2015). Carbonatite, igneous rock composed of > 50% magmatic carbonate minerals, was not recognized as an igneous lithology until the mid-twentieth century (Wyllie and Tuttle, 1960). Carbonatites and their associated silicate rocks have been identified around the world at craton margins and failed rift zones (Heaman et al., 2004; Jelsma et al., 2009) (Fig. 1a). The known occurrence of carbonatites is much higher in arid regions than in humid regions (Fig. 1a), which is probably an artifact of the difficulty of identifying these rocks in humid regions. Humid environments increase the extent of weathering and can lead to thick weathering profile and laterite formation. In the case of carbonatites, numerous mineral assemblages can result from different degrees of weathering, ranging from recrystalised carbonates and preserved primary minerals to sulphates, clays, oxides and chalcedony (Lottermoser, 1990). Considering this, research into the alteration/weathering mineralogy and remote detection of carbonatites and associated lithologies among sedimentary carbonates and in humid regions has the potential for new discoveries. Detection and mapping of carbonatite complexes is important for advancing the understanding of their petrogenesis and for evaluating their resource potential.

Carbonatites are found in association with and gradational between various silicate lithologies (Bailey, 1993; Mitchell, 2005) and present diverse facies given the complicated, rapid and deep rooted emplacement (Mitchell, 1986). Surface exposures of carbonatites are subject to these genetic and structural complexities as well as variable post emplacement alteration and country rock interaction (Shavers et al., 2016). Understanding the various conditions of surface exposures is essential to carbonatite mapping and may provide insight into textural and mineralogical differences between carbonatite genesis types. There has been some documentation of the weathering products of carbonatites yet these most often deal with nephelinite-clan carbonatites

* Corresponding author at: Department of Earth and Atmospheric Sciences, Saint Louis University, 3642 Lindell Blvd., Saint Louis, MO, 63108, USA.
E-mail addresses: ejshavers@gmail.com (E.J. Shavers), awulamu@slu.edu (A. Ghulam), encarnjp@slu.edu (J. Encarnacion).

https://doi.org/10.1016/j.oregeorev.2017.11.002
Received 21 December 2016; Received in revised form 8 August 2017; Accepted 4 November 2017
Available online 06 November 2017
0169-1368/

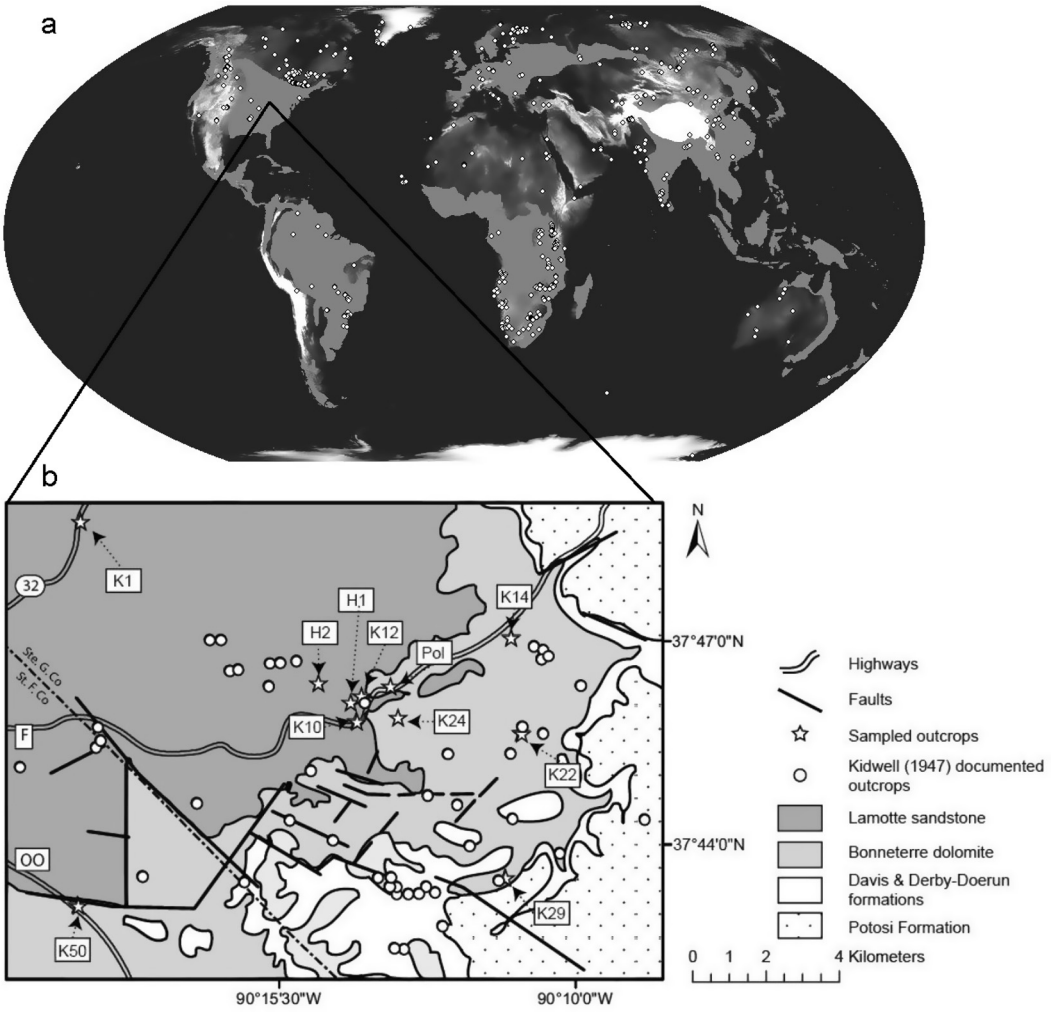

Fig. 1. a) Global distribution of carbonatites (white points) (Woolley and Kjarsgaard, 2008). Humid and tropical regions are identified by solid grey fill (National Geographic, 2005). Base map modified from ESRI (2016). b) The Avon Volcanic District (Shavers et al., 2016) with all documented intrusive outcrops plotted. Ste. G. Co- Ste. Genevieve County, St. F. Co- St. Francois County.

(Chakhmouradian et al., 2015; Walter et al., 1995) and the mineralogy of REE-bearing minerals (Sarapää et al., 2013; Xie et al., 2015).

In this study, samples of igneous and sedimentary lithologies have been collected from 12 outcrops in the Avon Volcanic District (AVD) (Fig. 1b), southeast Missouri, USA. The AVD intrusive lithologies grade between calciocarbonatite breccia, alnöite, and olivine melilitite. The associated dikes and pipes appear to have erupted during reactivation of mid-continent rift fractures in the early to middle Devonian (Shavers et al., 2017). Country rock in the AVD is mainly Cambrian sedimentary carbonates and sandstone. Identification of igneous carbonates in this context is challenging and limited outcrop exposure coupled with weathering and hydrothermal alteration compound the challenges. The geologic and geographic setting of the AVD make it an ideal area for the study of igneous/sedimentary carbonate differentiation. Results of this work are an extension of Shavers (2017) and contribute to carbonatite classification and the ongoing mapping of intrusives in the AVD. Mapping and exploration for AUC complexes typically involves extensive field and laboratory work that is often time-consuming and expensive. The work presented here documents unique primary and weathering mineralogy of the igneous carbonates and tests methods for remote characterization of AUC lithologies in fragile ecosystems that can reduce financial and scheduling costs. Normalized difference spectral index (NDSI) and chemometric methods are used to identify visible to short wave infrared (Vis-SWIR) reflectance bands unique to the intrusive carbonatites and these are attributed to specific mineralogies that cause the energy interaction. While many minerals do not have prominent reflectance features in the region, some mafic mineral alteration products do have recognized absorption features (Bedini, 2009; Rowan and Mars, 2003). In the Vis-Near-Infrared (NIR) region, several absorption features related to transition element content, valence state, and coordination are distinctive.

2. Past work on AUC spectroscopy

In their seminal series of articles on mineral Vis-SWIR spectroscopy, Graham Hunt and his associates review past work and present it alongside in-depth measurements of the reflectance and absorption features unique to many rocks and minerals (Hunt and Wynn, 1979; Hunt, 1977; Hunt and Salisbury, 1971; Hunt and Ashley, 1979; Hunt and Evarts, 1981; Hunt et al., 1973, 1974). Hunt et al. (1974) present spectra in the 325–2500 nm region for ultrabasic and basic rocks. Reflectance features for basic rocks are limited to a weak broad Fe signature centered near 1000 nm. Nonetheless, it is suggested by Hunt et al. (1974) that the ultrabasic reflectance signature is well defined and unique enough that “Typically… there is never any difficulty in distinguishing between ultrabasic and other rock types”. The features noted are well defined troughs near 1000 and 1800 nm, although the later would normally be difficult to distinguish because of the water absorption around 1900 nm. Iron in olivine and pyroxene can both contribute to the 1000 nm trough.

In their series *Visible and Near-Infrared Spectra of Minerals and Rocks*, Hunt and Salisbury (1971) analyze carbonate spectra. Observations of value include 5 bands in the short wave infrared region caused by the presence of CO_3 and several bands in the shorter wave lengths due to ferrous and ferric iron respectively. The carbonate bands are represented by absorption features centered near 1860, 1980, 2130, 2140, 2330, and 2530 nm. The common substitute of Fe for metal ions in carbonates lends to several reflectance features. Ferrous Fe often causes a broad feature near 1100 nm and Fe^{3+} can lead to features near 400, 700 and 870 nm given specific crystal structure and coordination. The authors suggest that subtle reflectance features can be detected for Fe content as low as 0.0005 wt%.

Several researchers have demonstrated the viability of using satellite and airborne Vis/NIR spectroscopy for AUC and carbonatite exploration. Bedini (2009) used HyMap data collected from an altitude of 2.5 km with 15–20 nm bandwidth, 126 bands between 440 and 2480 nm, and 4 m spatial resolution to map the Sarfartoq carbonatite complex of south-west Greenland. The resulting geologic map differentiates between "carbonatite, carbonatite outer core zone (fenite with carbonatite dykes), fenite, marginal alteration zone (hematized gneiss), gneiss" (Bedini, 2009), and vegetated areas. Field validation of 81 sites in the area indicates an accuracy of 87.6%. Bedini (2009) notes that Fe absorption features in the 1000–1300 nm range as well as carbonate features between 2320 and 2340 nm are important for differentiation. The shift of the CO_3 feature from 2320 to 2340 nm was indicative of the calciocarbonatite. The study area provided relatively undisturbed lithology exposures with little vegetation.

Bowers and Rowan (1996) employed AVIRIS data, collected from an altitude of ~18 km between 400 and 2500 nm with 224 channels and 16–20 m spatial resolution, in a similar pursuit, mapping the Ice River Alkaline Complex of Canada's British Columbia. In their work, the identification of ultramafic rocks along with a carbonatite phase and, like our study area, carbonate country rock is investigated. They report differentiation of 5 country rock subgroups and individual intrusive lithologies, primarily-ijolite mafic and primarily-magnesian carbonatite. The authors report that Al and Mg hydroxide bonds and CO_3 with features between 2190 and 2350 nm and Fe features between 800 and 1300 nm were the significant identifiers of separate lithologies. Bowers and Rowan (1996) identify differences between carbonate species but do not address the difference between magnesian carbonates of different petrogenesis as is the case in the AVD.

Galvão et al. (1995) studied AUC laterites in northern Brazil. The study is limited to correlation between spectra and phosphate, Fe, and Ti content using 19 spectra. Overall albedo and intensity of a Fe absorption feature highlight the variability in chemical content and allow discrimination between Al phosphate and Ti-rich laterites. These studies along with many others indicate the spectral sensitivity available for mineral and rock identification using imaging spectroscopy.

3. Study area

The study area for this work is the Avon Volcanic District (AVD), southeast Missouri, USA (Fig. 1). This region is host to a mid-Devonian ultramafic-carbonatite dike and diatreme complex (Shavers et al., 2016). The AVD is adjacent to and penecontemporaneous with the first known activity on the Ste. Genevieve Fault Zone which is perpendicular to, and terminates at, the Reelfoot Rift (Nelson et al., 1985). Country rock in the area is Paleozoic sedimentary dolomitic rock with sandstone found in the north-west portion of the AVD (Fig. 1b) and some outcropping Precambrian basement granite (Kidwell, 1947). Mapping of AVD intrusive dikes and pipes is ongoing yet hindered by vegetation, weathering, and surface exposure similarity to the country rock.

The AVD intrusive lithologies include and grade between olivine melilitite, alnöite, carbonatite, and carbonate-rich breccia (Fig. 2). These rocks outcrop in various forms and facies. The outcrop size can range from meter-scale knobs to dikes exposed for > 100 m. The rocks are more resistant than the country rock in some cases, retaining much of the primary mineralogy and igneous texture, and in others can be completely laterized and preferentially eroded. The later style has thus far only been found in the northwest quadrant of the AVD among the Lamotte Sandstone (K1 and H2 in Fig. 1b). The two laterized facies outcrops are from similar intrusive lithologies yet have different visual and chemical characteristics indicating that the laterization is not dependent on original mineralogy and more likely a feature of emplacement environment. Laterization can lead to concentrations of important elements (Lottermoser, 1990).

The AVD intrusive outcrops vary according to gradation among lithologies and their proportion of primary minerals. Mafics and carbonates are the dominant minerals. The primary mineralogy of the outcrop can have a great effect on the exposed facies. Rocks with a large proportion of mafic minerals that are easily altered will have higher proportions of alteration products such as carbonates, clays, and oxides. The spatial distribution of the lithologies relative to each other appears to be random aside from the K24 outcrop where alnöite and carbonatite rocks are both found. Carbonatite outcrops are predominantly calcite and dolomite along with the products of mafic mineral hydrothermal alteration, primary oxides, and garnet. The alnöite mineralogy is dominated by olivine, andradite garnet, and calcite. The olivine melilite outcrops found are generally primary olivine and melilite hydrothermally altered to calcite, clays, and oxides (Shavers et al., 2016).

4. Methods and materials

In the course of this study, spectral and rock samples were collected from 12 intrusive outcrops and adjacent sedimentary outcrops in the AVD. The hand samples were subjected to lithographic (Shavers et al., 2016) and powder X-ray diffraction (XRD) analysis in order to determine the weathering mineralogy. Laboratory spectroscopic reflectance measurements were made of weathered surfaces. The spectral data was analyzed for correlation with mineralogy using chemometric modeling, and automated index evaluation. Petrographic and whole rock geochemical data from a previous study (Shavers et al., 2016) are built upon.

4.1. X-ray diffraction analysis

Samples selected for petrographic and XRD analysis where selected to represent the lithologic gradation among carbonate-rich lithologies. The XRD powder preparation was adapted from Hillier (1999) and Srodon et al. (2001), detailed by Shavers et al. (2016), for the majority of the samples while some samples were only ground and sieved to < 250 μm. Analyses of the resulting powder was performed with a Bruker d8 Advance X-ray Diffractometer at the Washington University in St. Louis XRD lab and a Rigaku XRD MiniFlex 600 at Saint Louis University. The 2θ range analyzed is between 5° and 70° with a 0.02 step size and 0.5 s dwell time for the Bruker and 1°/min speed for the Rigaku. The more extensive XRD analyses revealed some minor phases not otherwise seen but for the most part the data was comparable between samples run using both methods. For clay mineral identification, we focused on the 5–20 2θ range because clays generally exhibit intense peaks in the region and there are few other mineral peaks that occur in that region (Moore and Reynolds, 1989).

4.2. Spectral analysis

The spectral wavelengths analyzed in this study are in the Vis-SWIR region, 350–2500 nm. In the field, spectral measurements were taken of weathered outcrop using a contact probe and the laboratory samples were measured using a bench probe. Both have a ~3.5 cm diameter window and are internally lit by a 5 W halogen lamp. The instrument used for spectral measurements is a PSR-3500 Spectroradiometer (Spectral Evolution, Inc.). The sampling spectral bandwidth is between

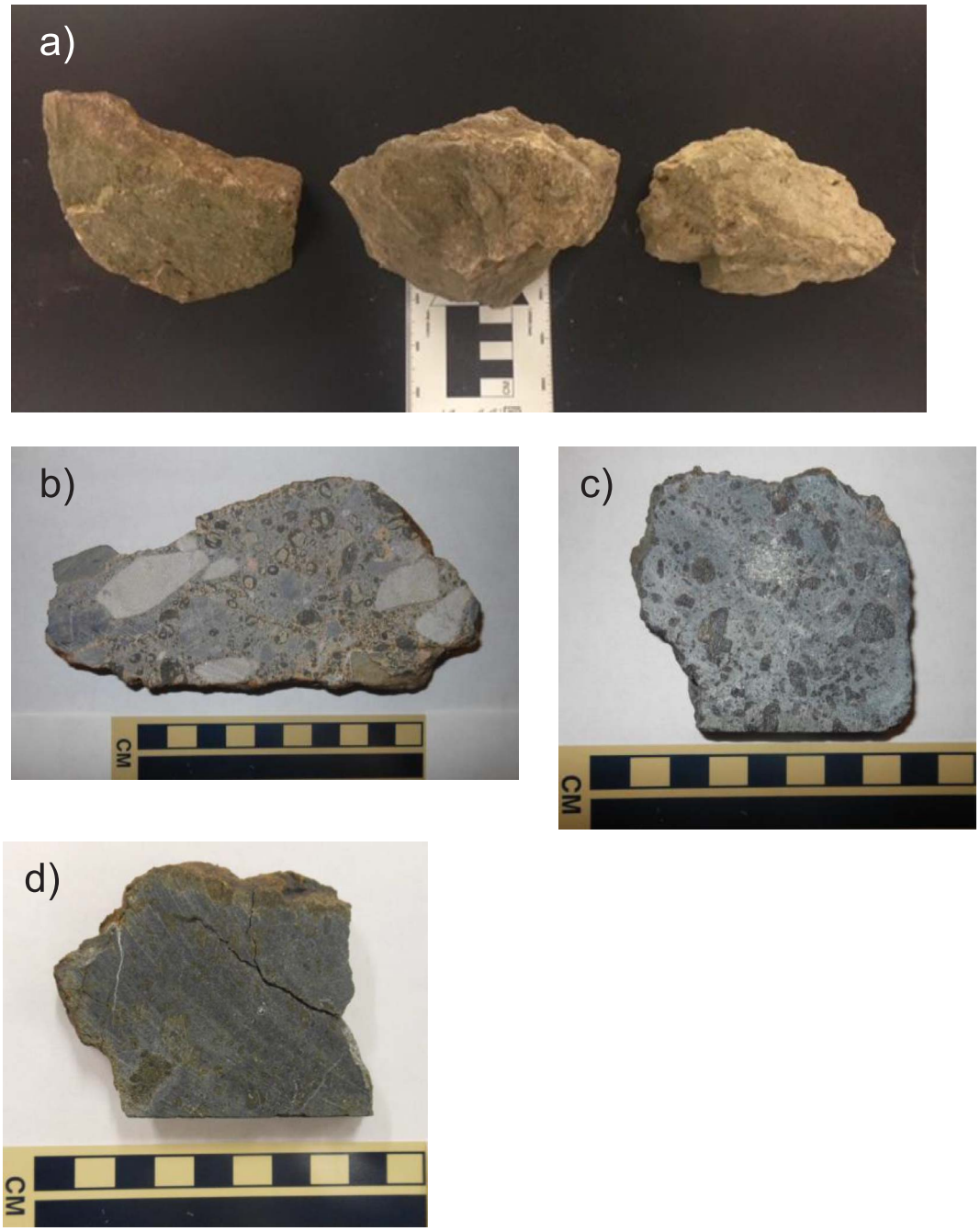

Fig. 2. AVD hand samples: a) carbonatite, metamorphosed carbonatite, and sedimentary dolomite taken from surface exposures. Slabbed hand samples: b) calciocarbonatite with sedimentary clasts, c) alnöite, d) olivine melilitite.

3 and 8 nm depending on wavelength. The measurements of individual samples were averaged to give representative curves for each lithologic facies. Spectra covering all the sampled outcrops were analyzed against mineral content and geochemistry to identify specific reflectance features unique to the intrusive lithologies. The resulting VIS-NIR reflectance and absorption features are tested for feasibility in remote detection scenarios.

In order to develop detection and quantification methods, several methods are implemented to determine the wavelengths most affected by the mineralogy, geochemistry and texture of the AVD lithologies. Important wavelengths for the various minerals found among the lithologies have been documented (Hunt, 1977; Hunt and Ashley, 1979), yet spectral mixtures and disordered lattice matrices are expected with the diverse compositions and parageneses found in the study area. Such features may lead to unique spectroscopic features that are indicative of AUC complexes and can be used in future remote detection.

4.2.1. Chemometric modeling

Chemometric modeling is a broad term that describes the use of chemical and spectral data in modeling the role of the chemical levels in the spectral response. The spectral data can be of various values and variables. Chemometric modeling is used in various disciplines (Frank and Friedman, 1993). The modeling provides insight into the chemical and molecular causes for the relative absorption and reflectance features. Understanding the causes of spectral features in the study area is of use in scaling up the methods to other regions which will vary in their chemistry and mineralogy. Whole rock chemical data is taken

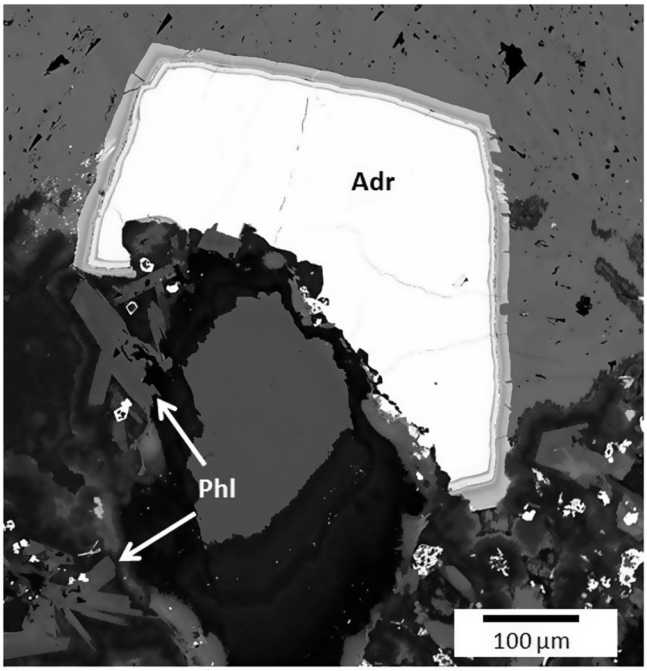

Fig. 3. Electron backscatter image of phlogopite (Phl) and andradite (Adr) phenocrysts in a matrix including calcite, silica, magnetite, serpentine, and chromite (small white areas).

from Shavers et al. (2016) and from ideal formulas given the respective mineralogy.

The modeling of chemical correlation with spectral response was done using the GRAMS IQ software (Thermo Fisher Scientific Inc.). The spectra from the PSR3500 collection interface are exported into the GRAMS IG software along with a file containing the geochemical data. The models tested are partial least squares (PLS) and principle component regression (PCR) analyses (Frank and Friedman, 1993). Once a model was developed with a strong correlation coefficient, a random subset of spectra was used to test the model.

4.2.2. Normalized difference spectral indices

The NDSI evaluation is a simple method of testing the correlation between normalized difference index (NDI) values $[(band1-band2)/(band1 + band2)]$ from the averaged spectra and chemical content (Stagakis et al., 2010). The benefit of the NDSI is that it is not sensitive to atmospheric and sensor geometry conveying variable curve geometries like peak heights and shoulders. A script was developed to implement the NDSI analysis by testing each wavelength (λ_x) against every other wavelength (λ_i) in a normalized difference index $[NDSI_{x,i}=(\lambda_x + \lambda_i)/(\lambda_x-\lambda_i)]$ and comparing these results to the chemical levels of the respective samples. The output includes the coefficient of determination (r^2) and p-value results.

5. Results and discussion

This study identifies mineralogical and spectral differences between the weathered facies of sedimentary and igneous carbonates of the AVD. The difference in bulk mineralogy between the igneous and sedimentary lithologies is usually not clearly discernable because the ratio of carbonate minerals to silicates is large (Shavers et al., 2016) and because of the similarity between sedimentary and weathered igneous mineralogies. Here we identify a minor mineral composition among the weathered surfaces that differentiates the AVD intrusives and is explained by the primary mineralogy and chemistry. The diverse minor mineralogy along with the sensitivity of Vis-SWIR spectroscopy to texture, grain size, and other factors make determination of exact mineralogy and causes of spectral features in reflectance measurements difficult. There are however general trends in the spectral response of weathered surfaces that allow for differentiation between igneous and sedimentary rocks in the AVD using optical remote sensing methods and some conclusions can be made given thermodynamic calculations in conjunction with mineralogy and geochemistry.

Although the mineralogy of the AVD carbonatites has unique constituents, not all minerals have electronic properties that produce noticeable reflectance or absorption features in the Vis-SWIR spectral range (Hunt, 1977). Proportion of minerals in the rocks also dictates whether they are perceptible using remote sensing techniques. Clay minerals, serpentine, and phlogopite all have molecular properties that cause absorption features in the Vis-SWIR range and have been identified in the AVD carbonatite weathering profile in proportions perceptible in field and lab spectra and likely with high resolution airborne spectroscopy. Titaniferrous melanite has been identified as a relict in an extensively weathered pipe and among other outcrops. There are absorption features in the longer wavelength visible regions that are attributed here to charge transfer between Fe and Ti and transition metal electronic transitions and may be useful for igneous carbonate differentiation. REE levels are elevated among AVD lithologies, REE mineralization has not been clearly identified yet may be found in minor phases undetected here such as allanite.

5.1. Weathering mineralogy

Minor constituent minerals have been identified in the altered surface mineralogy of the AVD carbonatites in an environment of variable weathering that differentiate carbonatites from sedimentary carbonates. These minerals have complicated formation pathways yet can be generally grouped into relict primary minerals and post-emplacement alteration products. The extent of weathering can range from unaltered olivine bearing ultramafic rock to laterite consisting of clay and quartz. The majority of the outcrops are moderately weathered with evidence of extensive hydrothermal interaction and small amounts of clay forming on mineral rims and interstitially.

5.1.1. Relict minerals

Phenocrysts of phlogopite can be visually identified in most AVD intrusive hand samples and petrographic analysis reveals phlogopite as present among nearly all of the 12 sampled outcrops (Fig. 3) (Shavers et al., 2016). Another mineral found in the weathered rock and considered primary in the AVD intrusives is Ti-rich andradite garnet. Andradite is found to be a significant component of the ultramafic alnöite dikes and pipes but is also found among the carbonatites in smaller proportions. Phlogopite and andradite are both relatively resistant to weathering to the point that they can be found as constituents of sand.

Chrome spinel is found to be resistant to weathering compared to ferromagnesian minerals and has been identified in petrographic analysis (Fig. 3). The spinel content is difficult to identify in the AVD XRD results because of overlap with carbonate peaks. In samples from K1, the most extensively laterized outcrop found in this study, the XRD analysis indicates the presence of franklinite, Zn spinel. Ilmenite may be another relict mineral with important Ti and Fe content yet the XRD patterns are not definitive because of the density of diffraction signals that overlap it.

5.1.2. Alteration products

Lizardite forms along with magnetite in retrograde metamorphism and alteration of olivine and is found in 7 outcrops. Lizardite is not found where hydrothermal alteration has led to carbonate replacement of most of the minerals or weathering is intensive. Magnetite and other oxides are inevitable components in this environment given the oxidation and elevated Fe levels (Table 1), yet they do not make up a significant portion of the mineralogy.

Chlorite is a common mineral found in weathering environments and in this study is the result of low temperature alteration of

Table 1
Major and minor element weight % oxide data for AVD lithologies from Shavers et al. (2016). The samples analyzed are relatively fresh and do not represent surface alteration.

Rock Type	Olivine Melilitite	Alnöite		Calciocarbonatite			
Sample ID	L9A2	L3F1	A62A	A63	L81	L62	L121
Outcrop ID	K22	K24	K10	Pol	K29	H1	K50
SiO2	31.68	32.46	35.43	29.39	26.14	42.61	32.42
Al2O3	5.38	5.55	5.7	4.57	4.54	4.34	3.99
Fe2O3	11.31	12.89	12.39	10.2	8.48	7.03	7.91
MnO	0.181	0.187	0.183	0.151	0.148	0.096	0.102
MgO	19.55	19.62	21.68	16.34	7	4.62	2.47
CaO	10.99	14.05	12.48	16.03	25.67	18.77	26.13
Na2O	0.12	0.4	0.19	0.18	0.06	0.22	0.18
K2O	0.42	0.71	1.16	0.44	0.13	1.34	0.39
TiO2	1.48	1.85	1.754	1.266	1.09	1.07	0.84
P205	0.48	0.65	0.67	1.27	0.28	0.59	0.43
Cr2O3	0.23	0.24	0.19	0.09	0.12	0.05	0.1
CO2	18.39	11.53	8.12	18.33	26.56	18.95	25.31
Total	100.3	100.3	99.75	98.17	100.3	99.75	100.4

Rock Type	Metasomatised carbonatite			Dolomitic country rock			Sandstone country rock
Sample ID	L2M	A66B	A64A	A62C	A66A	L111	L56
Outcrop ID	K10	K12	K24	K10	K12	K50	K1
SiO2	16.37	35.86	12.26	11.69	5.42	18.38	94.02
Al2O3	2.97	3.52	4.32	3.37	1.39	3.36	0.65
Fe2O3	5.4	3.44	5.16	2.75	2.72	5.71	1.04
MnO	0.152	0.177	0.162	0.237	0.338	0.314	0.017
MgO	16.17	9.67	15.43	16.35	18.31	14.63	0.71
CaO	22.7	17.57	24.42	25.57	28.61	21.94	0.73
Na2O	0.17	0.1	0.2	0.15	0.08	0.22	0.08
K2O	0.51	2.15	0.88	0.88	0.17	1.58	0.15
TiO2	0.78	1.005	1.07	0.17	0.09	0.16	0.13
P205	0.39	1.01	0.48	0.19	0.07	0.18	0.03
Cr2O3	0.06	0.02	0.13	0.03	0	0.03	0.02
CO2	33.87	23.84	34.56	37.81	42.34	33.46	1.06
Total	99.6	98.34	99.16	99.22	99.56	99.98	98.65

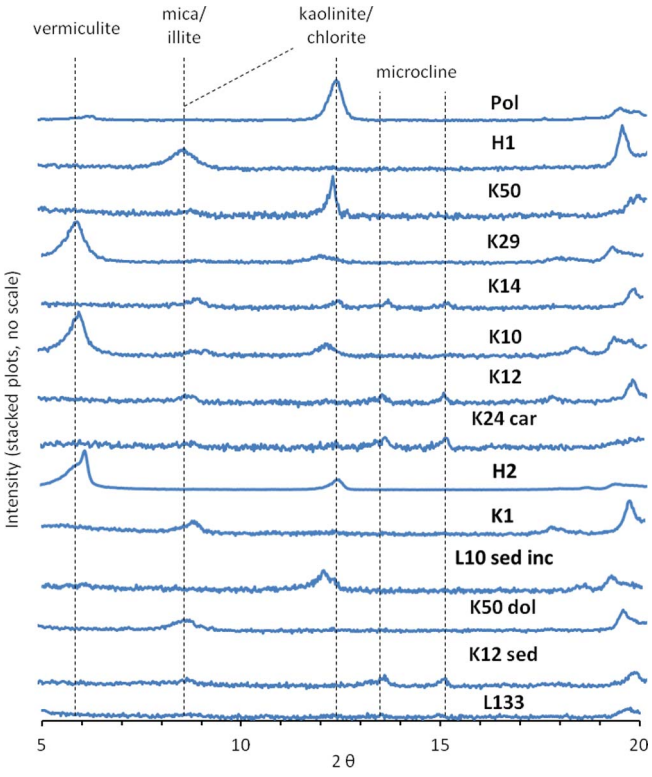

Fig. 4. Plot of AVD XRD results, the sample name is listed at right. Calciocarbonatites: Pol, H1, K50, K29, K14; altered carbonatites: K10, K12, K24 car; laterized intrusives: H2, K1; dolomitic country rock: K50 dol, K12 sed, L133; sedimentary clast from a breccia: L10 sed Inc.

ferromagnesian primary minerals. The presence of chlorite is confirmed by petrographic and XRD analysis (Fig. 4). Levels are high enough for XRD detection in only four of the samples studied. The samples in which chlorite is found are in various states of alteration.

All of the outcrops with moderate to extensive alteration have clay mineral components detectable in thin section and hand sample. This is not always discernible in XRD analysis of samples that have not been subjected to clay mineral separation. Nonetheless, clay signatures have been identified in 6 of the samples analyzed giving a reasonable approximation of the mineralogy in samples with lower clay proportions.

Two of the outcrops subject to XRD analysis have discernible illite content. Illite is a K-Al sheet silicate often formed with the weathering of feldspars but it can also be found in regions of hydrothermal alteration. The AVD rocks have been shown to have likely had a significant water-rich fluid phase alter the mineralogy (Shavers et al., 2016). Yet, the outcrops found to contain significant illite differ in lithology and degree of alteration suggesting the presence of illite among the outcrops is subject more to potassium content. One of the illite-bearing samples (A66B) has the highest K2O wt% found among the intrusive lithologies in this study (Table 1) and the other (K1) is the most extensively laterized sample found in the course of this study.

Another clay mineral found to be significant in the intrusive rock weathering mineralogy is vermiculite. The vermiculite signature was identified in three XRD patterns for the AVD intrusives with alteration ranging from moderate to extensive. The samples found with vermiculite appear to have higher combined Fe, Mg, Al, and Ca, than the other rocks with moderate to significant alteration. These elements are the principle metals occupying the cation sites of vermiculite. There is also a Fe and Mg-rich muscovite (celadonite) that has been indicated from XRD analysis of the K1 site samples. Muscovite is a common product of hydrothermal alteration, including in ore zones and has been used as an indicator mineral in studies of remote sensing of ore deposits

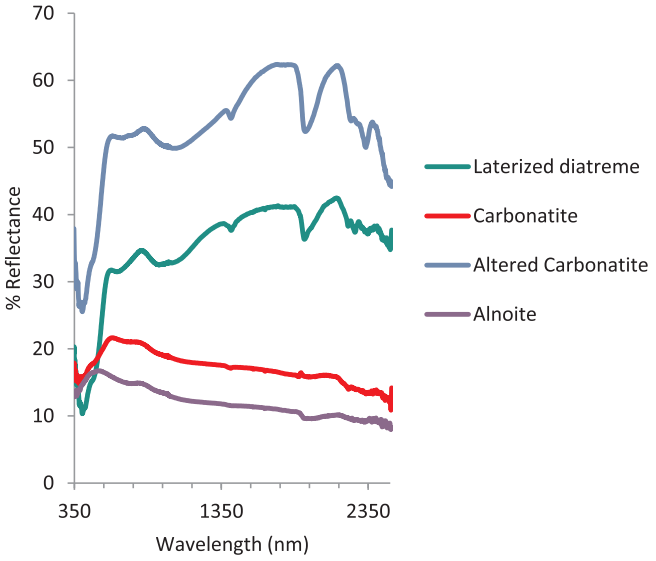

Fig. 5. Sample reflectance curves from AVD intrusive lithologies.

(Buckingham and Sommer, 1983; Kruse et al., 2012).

5.2. Spectroscopic results

The weathering mineralogy of the AVD outcrops has been documented here as well as a remote sensing model for the discrimination of carbonatite complexes among carbonate country rock and environments prone to extensive surface alteration due to weathering. In this work, two methods are investigated with the aim of identifying lithology unique spectroscopic reflectance features in the Vis-SWIR spectral region (Fig. 5). Chemometric modeling of AVD spectra using geochemical data from the study by Shavers et al. (2016) is developed to identify regions of the spectra that correlate with AVD chemistry. The models developed confirm the SWIR region between 2100 and 2400 nm as valuable in identifying igneous carbonates (Fig. 6). Interestingly, the model also suggests minor element components may lead to unique features in the visible region. Finally, a NDSI model is used to test the potential for index use in remote sensing (Inoue et al., 2008). The NDSI supports the above findings including the visible region potential importance.

5.2.1. Chemometric results

The chemometric analysis of the AVD reflectance spectra led to the identification of band regions of interest in the Vis-NIR and SWIR wavelengths. Multiple statistical treatments where applied to optimize the modeling of the spectral response to chemical content. The coefficient of correlation and factor weights were used to identify regions of the spectra related to the chemistry. In the Vis-NIR region there are three broad absorption features that are well defined among the intrusive rocks and narrower visible region features among some. Both major and trace element chemistry were tested against the spectral data.

In the Vis-NIR region, Ni and Cr have the highest correlation with the spectral data among the trace elements. Both of these transition elements have the potential to produce electronic transition induced absorption features in this region. While correlation coefficients are high for Ni and Cr, correlation between the trace elements and Fe make the causation difficult to determine. For both, the factor weights are highest in the 860 nm region although the weights plot is extremely noisy when narrowed in on the region beyond the 400–1300 nm swath (Fig. 6). The coefficient of correlation for Ti reached $R^2 = 0.81$ when the spectral region was narrowed to 600–750 nm. Narrowing or shifting the region from this range generally was deleterious. We attribute the intensity of the feature centered around 650 nm to the presence of ~7 wt/% Ti oxide in andradite and charge transfer with Fe which can exist as ferric or ferrous in the octahedral and tetrahedral sites (Huggins et al., 1977a). Divalent Ni in lizardite and spinel may also contribute to

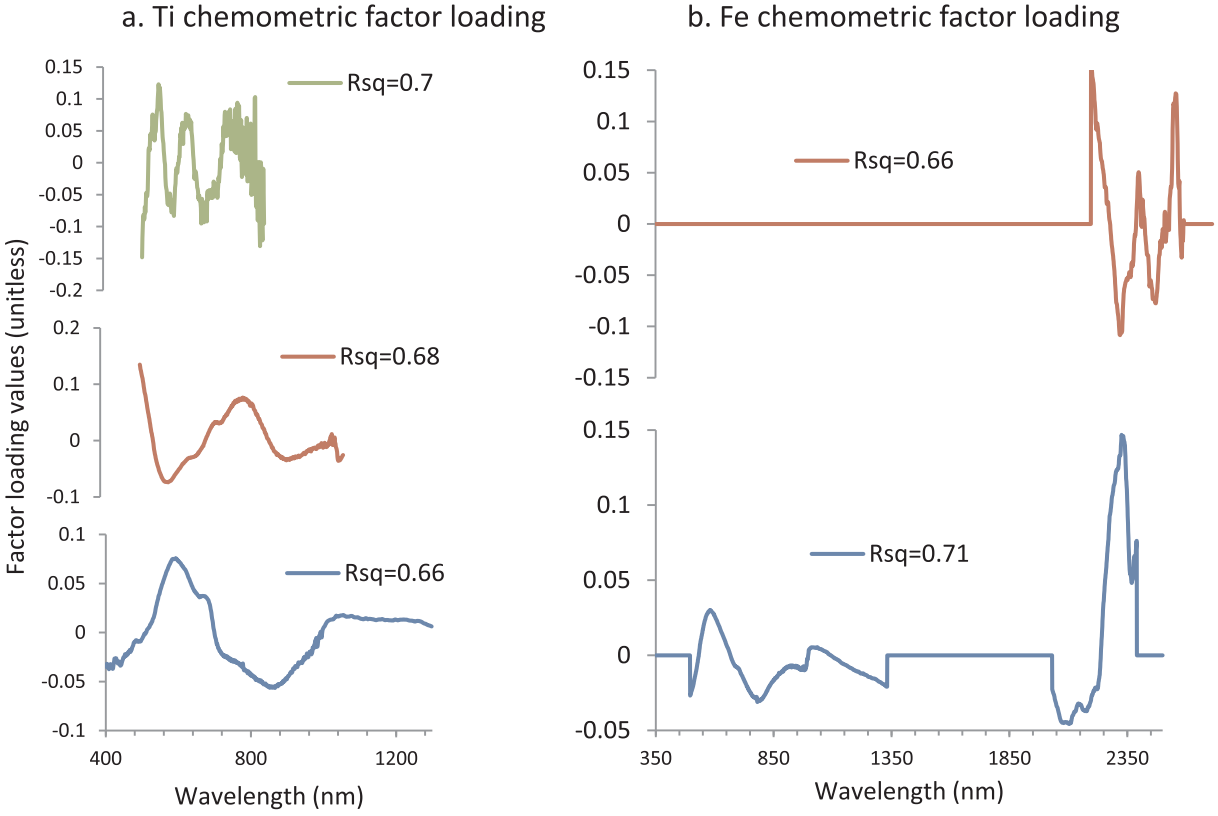

Fig. 6. Factor loading plots from the chemometric analysis.

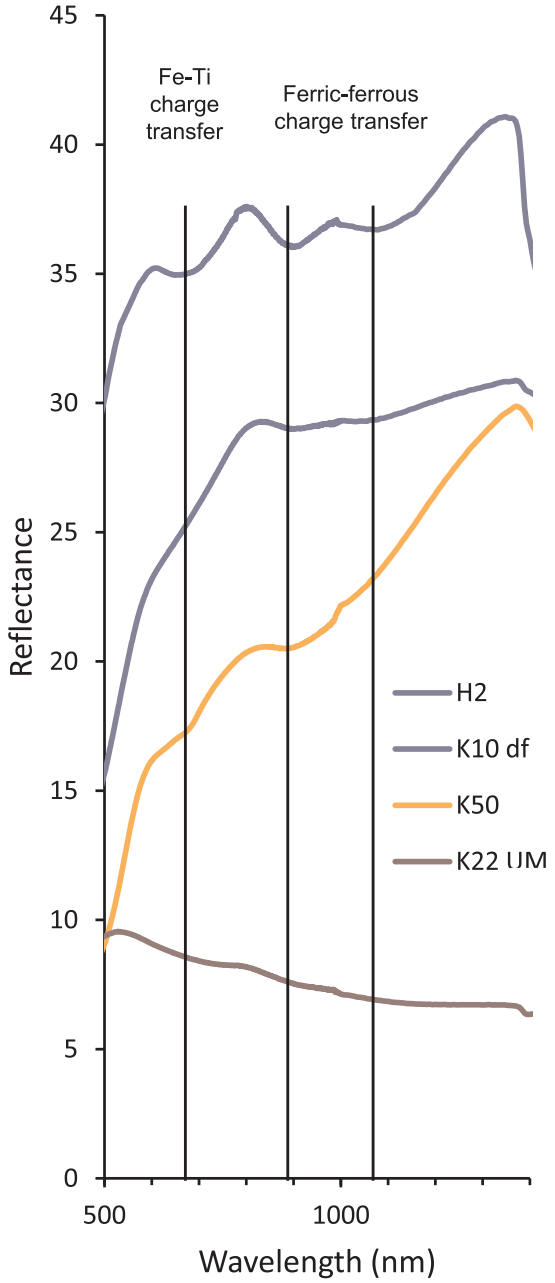

Fig. 7. Vis-NIR reflectance spectra from intrusive rocks indicating the Fe and Ti absorption features. H2 – laterized carbonatite, K10 – altered carbonatite, K50 – carbonatite, K22_UM – olivine melilitite.

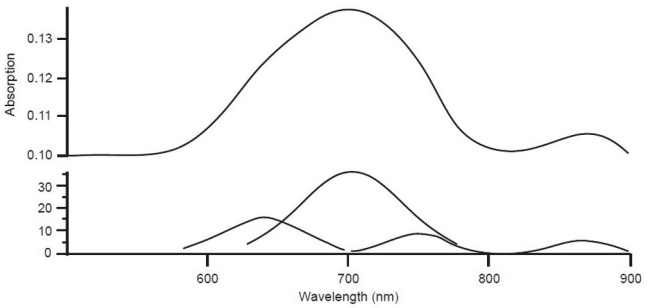

Fig. 8. Plot of sample H2, laterized diatreme facies, inverted with continuum removed. Gaussian curve fitting was performed in the IgorPro software.

this feature (Hunt, 1977). The total Fe content shows strong correlation in the Vis-NIR region yet is more common in sedimentary lithologies than Ti and the trace elements and therefore of less use in remote classification.

Melanite is present among the weathered crusts of outcrops and is primary in the intrusive AVD lithologies. The chemometric spectra analysis clearly points to the visible region of the AVD igneous lithology reflectance spectra for evidence of unique spectral identifiers. The broad band in the 650–700 nm region is unique to igneous lithologies and most evident among those where melanite is abundant. Absorption features in the longer wavelength visible region resulting from the crystal field splitting of the 3d1 Ti^{3+} cation in a distorted octahedral have been documented by others (Dowty and Clark, 1973; Khomenko et al., 1994; Prewitt et al., 1972). Yet the balancing of the melanite formula indicates that Ti^{4+} is the dominant valence state in order to balance the charge given trivalent (and possibly divalent) Fe occupying roughly half of the tetrahedral sites. Fe preferential occupies the tetrahedral site over Ti (Huggins et al., 1977b). The feature is a broad (50 nm) shallow absorption band evident in many igneous AVD AUC spectra and well defined in the spectra from outcrops with ultramafic minerals present which are dominated by olivine, serpentine, and titaniferous andradite. A 700 nm absorption band is a common feature of ferric-ferrous charge transfer and is overlapping the 650 feature here (Figs. 7 and 8).

There are ferric and ferrous absorption features identified in the mineralogy and spectra of the AVD intrusives. Sharp features in the 400–600 nm region of spectra from fresh slabbed samples are associated with ferrous Fe while ferric Fe can lead to features throughout the Vis-NIR region, although less prominent in the shorter wave lengths. Iron is found in many phases in the intrusive rocks including phlogopite, andradite, melanite, olivine, and oxides. The sharp features are not always detectable in the weathered surface spectra (Fig. 7) where the Vis-NIR region is dominated by several broader features. These features are centered around 680, 900 and 1100 nm and attributed here primarily to charge transfer between transition elements. The absence of these features in sedimentary rocks with comparable Fe content is likely due to the Fe being found in dolomite.

In the SWIR region, the 2000–2500 nm region is clearly useful in detecting carbonate rocks because of the strong and dominant carbonate ion vibrational features in the region (Gaffey, 1985; Hunt and Salisbury, 1971). The chemometric modeling points to a narrower SWIR region as strongly correlated with the chemistry (Fig. 6). In the 2180–2400 nm region, the igneous lithologies display a more intense absorption feature in the 2200–2300 nm region than the sedimentary rocks. This amplification is attributed here to the presence of Mg in serpentine and phlogopite in the intrusive rocks. The NDSI indicates that an index using bands in this region may be useful in differentiating igneous carbonates and associated lithologies among sedimentary rocks of similar mineralogy.

5.2.2. *Normalized difference spectral index*

The NDSI test of index correlation with whole rock geochemistry was run against the major and minor element oxide wt% (Table 1). The results of the NDSI show a strong correlation between bands in the short wave IR region and the AVD geochemistry (Fig. 9). The Vis-NIR region shows only narrow regions with moderate correlation. The shorter wavelength visible region shows moderate to good correlation with several chemical constituents. The ratio between the 500 and 350 nm regions stands out for Al, Fe, and Ti oxides, yet the spectra signal to noise ratio in this region can be low making the range less useful for remote detection.

Similar to the chemometric modeling results, Ti has the strongest correlation among the minor constituents. Correlation coefficients near 0.8 in two distinct regions of the SWIR region and are strong in the 350–550 nm region. The Al oxide values appear to correlate with similar regions. The correlation coefficients reach 0.68 in the SWIR

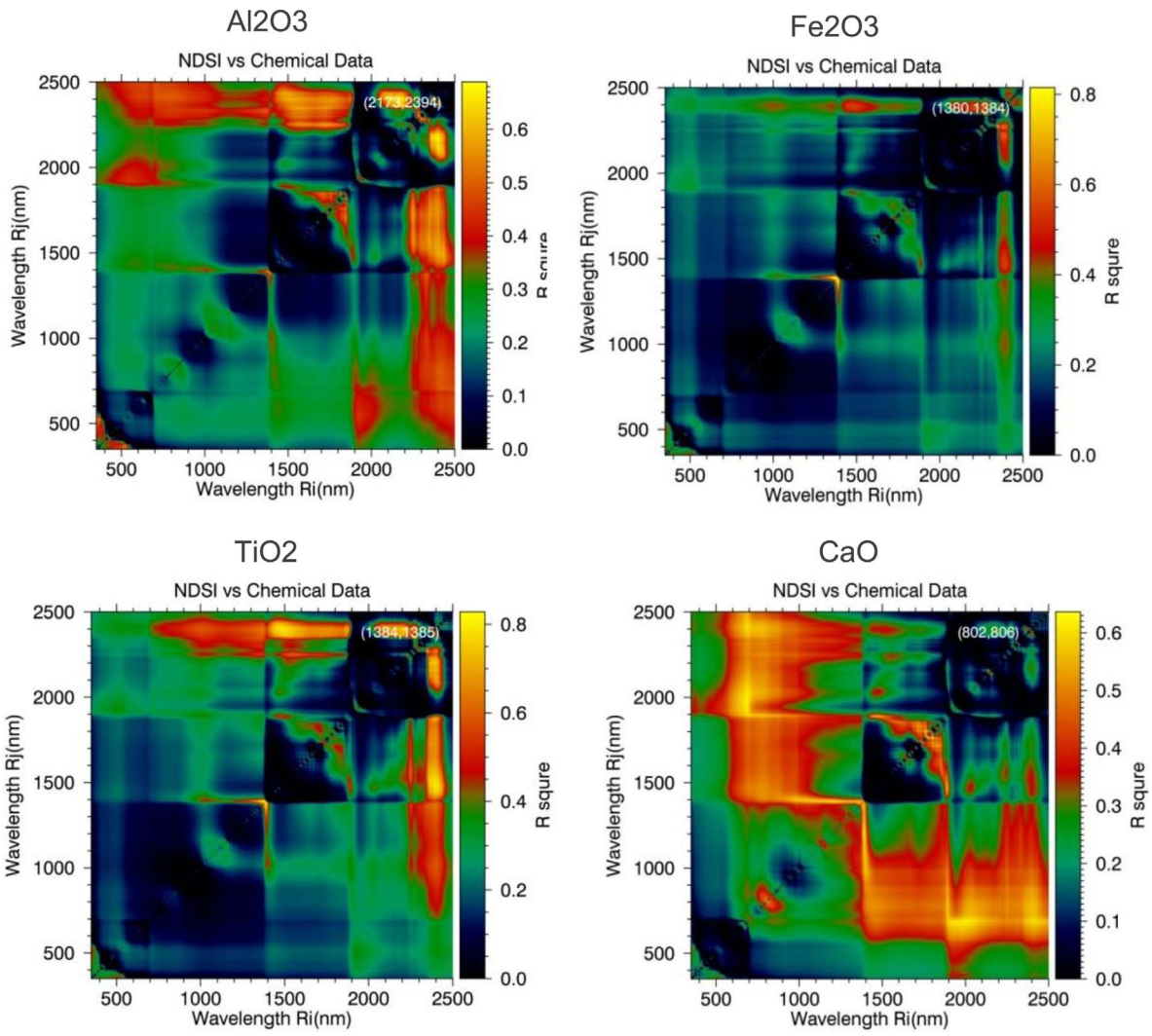

Fig. 9. Results plots from the Normalized Difference Spectral Index analysis.

region and show potential in the same 350–550 nm region.

Along with Ti, Fe oxide values show the strongest correlation to the NDSI-developed ratios. The areas that appear to be important for Ti and Al content prediction often overlap with the regions that correlate with Fe content. As was noted in Section 5.2.1, Fe correlates strongly with many of the minor and trace elements and is likely the cause of much of the spectral response to AVD geochemistry.

The visible region band index for 500 and 350 nm shows potential for Ti, Al, and Fe measurement. This is likely a reflection of the shoulder in this region attributed to charge transfer in hydroxides causing the steep drop off. Minerals with Fe, Al, and Ti are capable of producing the intense drop off in the hydroxide scenario that are common to weathering minerals (Hunt, 1977).

The correlation coefficients for Ca show some potential for index evaluation of mineralogy. The bands indicated as index components are unique in this experiment. The strongest correlation is found using bands in the 675 and 1900–2400 nm regions. This is a logical spectral response given the strength of the absorption features in the SWIR region. An index using these bands may be best suited to differentiation among carbonatites of varying lithologies where the Fe, Al, and Ti content may be similar yet the carbonate species vary.

6. Conclusion

We have identified weathering mineralogy of igneous and sedimentary lithologies and spectral reflectance features in the Vis-SWIR regions that are unique to intrusive carbonatites. The bulk mineralogy of the AVD carbonate rocks is very similar, yet lithographic and XRD analyses have been applied to identify lizardite, vermiculite, phlogopite, and melanite as unique minor phases in intrusive carbonates. Chlorite and muscovite are more common in moderately altered intrusive rocks than in other outcrops yet these minerals are also present among some sedimentary lithologies and thus not as useful for differentiation of carbonate petrogenesis.

Chemometric modeling and NDSI analysis of weathered surface Vis-SWIR reflectance spectra have been used to determine the feasibility of remote differentiation of igneous and sedimentary carbonates in humid regions. The spectral analyses point to two regions as important for lithology identification. In the Vis-NIR region, the 650–700 nm region correlates strongly with trace element Cr and Ni as well as Fe and Ti. The broad absorption found here in intrusive carbonates is attributed to charge transfer between Fe and Ti and influenced by Ni crystal field splitting in lizardite and spinel as well as Fe in several phases. In the SWIR region, the carbonate feature centered near 2250 nm is more intense among the intrusive rocks. The increased intensity is likely due to the presence of magnesian lizardite and phlogopite and higher Mg content in general.

The spectral features found here show that there is a strong potential for remote detection of carbonatites and associated ore deposits in humid regions subject to varying surficial weathering, even among

sedimentary carbonates. The low ratio of the indicator minerals within the carbonatite lithologies and their complex reflectance signatures make high spatial and spectral resolution remote sensing data ideal for remote mapping in the study area. The hyperspectral Hyperion instrument on the EO-1 spacecraft has 5 bands centered in the 650–700 nm region and 3 centered near 2244, 2254, and 2264 nm that could potentially differentiate the igneous carbonates. Yet, the 30-meter resolution spatial resolution would prove challenging given the small outcrop size and vegetation. Future work will apply these findings to high-resolution hyperspectral data collected from an unmanned aerial vehicle (UAV) platform.

The spectral signatures of carbonatite alteration products identified in the AVD can be used to identify altered ultramafic-associated carbonatites elsewhere. Aillikite, kimberlite, and melilitite-clan carbonatites all feature mineralogies with the potential to produce spectral features similar to the AVD.

Acknowledgments

We are grateful to the editor and reviewers of this journal. This work was supported financially by the Geological Society of America (10377-14) and the Saint Louis University Center for Sustainability. We thank Pat Mulvany for consultation and guidance in the field. We are grateful to Paul Carpenter for assistance with microprobe analysis at Washington University in Saint Louis. This work is an extension of doctoral dissertation work done by the first author (Shavers, 2017).

References

Bailey, D.K., 1993. Carbonate magmas. J. Geol. Soc. 150 (4), 637–651.
Bedini, E., 2009. Mapping lithology of the Sarfartoq carbonatite complex, southern West Greenland, using HyMap imaging spectrometer data. Remote Sens. Environ. 113 (6), 1208–1219.
Bowers, T.L., Rowen, R.C., 1996. Remote Mineralogic and Lithologic Mapping of the Ice River Alkaline Complex, British Columbia, Canada, Using AVIRIS Data Photogrammetric Engineering and Remote Sensing, 62, 1379–1385.
Buckingham, W.F., Sommer, S.E., 1983. Mineralogical characterization of rock surfaces formed by hydrothermal alteration and weathering; application to remote sensing. Econ. Geol. 78 (4), 664–674.
Chakhmouradian, A.R., Reguir, E.P., Kressall, R.D., Crozier, J., Pisiak, L.K., Sidhu, R., Yang, P., 2015. Carbonatite-hosted niobium deposit at Aley, northern British Columbia (Canada): mineralogy, geochemistry and petrogenesis. Ore Geol. Rev. 64, 642–666.
Dowty, E., Clark, J., 1973. Crystal structure refinement and optical properties of a Ti3+ fassaite from the Allende meteorite. Am. Mineral. 58, 230–242.
ESRI, 2016. Global Terrain Data.
Frank, L.E., Friedman, J.H., 1993. A statistical view of some chemometrics regression tools. Technometrics 35 (2), 109–135.
Gaffey, S.J., 1985. Reflectance spectroscopy in the visible and near-infrared (0.35–2.55 μm): applications in carbonate petrology. Geology 13 (4), 270–273.
Galvão, L.S., Vitorello, Í., Paradella, W.R., 1995. Spectroradiometric discrimination of laterites with principal components analysis and additive modeling. Remote Sens. Environ. 53 (2), 70–75.
National Geographic, 2005. Climate Zones Simplified- Robinson.
Giuliani, A., Phillips, D., Kamenetsky, V.S., Goemann, K., 2015. Constraints on kimberlite ascent mechanisms revealed by phlogopite compositions in kimberlites and mantle xenoliths. Lithos 240–243, 189–201.
Heaman, L.M., Kjarsgaard, B.A., Creaser, R.A., 2004. The temporal evolution of North American kimberlite. Lithos 76 (1–4), 377–397.
Hillier, S., 1999. Use of an air brush to spray dry samples for X-ray powder diffraction. Clay Miner. 34 (1), 127–135.
Huggins, F., Virgo, D., Huckenholz, H., 1977. Titanium-containing silicate garnet; I, the distribution of Al, Fe (super 3+), and Ti (super 4+) between octahedral and tetrahedral sites. Am. Mineral. 62 (5–6), 475–490.
Huggins, F., Virgo, D., Huckenholz, H., 1977. Titanium-containing silicate garnets; II, the crystal chemistry of melanites and schorlomites. Am. Mineral. 62 (7–8), 646–665.
Hunt, G., Wynn, J., 1979. Visible and near-infrared spectra of rocks from chromium-rich areas. Geophysics 44 (4), 820–825.
Hunt, G.R., 1977. Spectral signatures of particulate minerals in the visible and near infrared. Geophysics 42 (3), 501–513.
Hunt, G.R., Salisbury, J.W., 1971. Visible and near-infrared spectra of minerals and rocks: II. Carbonates. Modern Geol. 2, 23–30.
Hunt, G.R., Ashley, R.P., 1979. Spectra of altered rocks in the visible and near infrared. Econ. Geol. 74 (7), 1613–1629.
Hunt, G.R., Evarts, R.C., 1981. The use of near-infrared spectroscopy to determine the degree of serpentinization of ultramafic rocks. Geophysics 46, 316–321.
Hunt, G.R., Salisbury, J.W., Lenhoff, C.J., 1973. Visible and near-infrared spectra of minerals and rocks: VII. Acidic igneous rocks. Modern Geol. 4, 217–224.
Hunt, G.R., Salisbury, J.W., Lenhoff, C.J., 1974. Visible and near infrared spectra of minerals and rocks: IX. Basic and ultrabasic igneous rocks. Modern Geol. 5, 15–22.
Inoue, Y., Peñuelas, J., Miyata, A., Mano, M., 2008. Normalized difference spectral indices for estimating photosynthetic efficiency and capacity at a canopy scale derived from hyperspectral and CO 2 flux measurements in rice. Remote Sens. Environ. 112 (1), 156–172.
Jelsma, H., Barnett, W., Richards, S., Lister, G., 2009. Tectonic setting of Kimberlites. Lithos 112, 155–165.
Jones, A.P., Genge, M., Carmody, L., 2013. Carbonate melts and carbonatites. Rev. Mineral. Geochem. 75 (1), 289–322.
Lottermoser, B., 1990. Rare-earth element mineralisation within the Mt. Weld carbonatite laterite, Western Australia. Lithos 24 (2), 151–167.
Khomenko, V., Langer, K., Andrut, M., Koch-Müller, M., Vishnevsky, A., 1994. Single crystal absorption spectra of synthetic Ti, Fe-substituted pyropes. Phys. Chem. Min. 21 (7), 434–440.
Kidwell A.L., 1947. Post-Devonian Igneous Activity in Southeastern Missouri, edited by M. D. o. B. a. Administration, Jefferson City, MO.
Kruse, F.A., Bedell, R.L., Taranik, J.V., Peppin, W.A., Weatherbee, O., Calvin, W.M., 2012. Mapping alteration minerals at prospect, outcrop and drill core scales using imaging spectrometry. Int. J. Remote Sens. 33 (6), 1780–1798.
Mitchell, R.H., 1986. Kimberlites: Mineralogy, Geochemistry, and Petrology. Plenum Press, London & New York xviii + 442p pp.
Mitchell, R.H., 2005. Carbonatites and carbonatites and carbonatites. Can. Mineral. 43 (6), 2049–2068.
Mitchell, R.H., 2008. Petrology of hypabyssal kimberlites: Relevance to primary magma compositions. J. Volcanol. Geoth. Res. 174 (1), 1–8.
Moore, D.M., Reynolds, R.C., 1989. X-Ray Diffraction and the Identification and Analysis of Clay Minerals. Oxford University Press, Oxford.
Nelson, W.J., Lumm, D.K., Schwalb, H.R., 1985. Ste. Genevieve fault zone, Missouri and Illinois, edited by U. S. N. R. C. Office of Nuclear Regulatory Research, Division of Radiation Programs and Earth Sciences, Washington, D.C.
Prewitt, C.T., Shannon, R.D., White, W.B., 1972. Synthesis of a pyroxene containing trivalent titanium. Contrib. Miner. Petrol. 35 (1), 77–82.
Rowan, L.C., Mars, J.C., 2003. Lithologic mapping in the Mountain Pass, California area using Advanced Spaceborne Thermal Emission and Reflection Radiometer (ASTER) data. Remote Sens. Environ. 84, 350–366.
Sarapää, O., Al Ani, T., Lahti, S.I., Lauri, L.S., Sarala, P., Torppa, A., Kontinen, A., 2013. Rare earth exploration potential in Finland. J. Geochem. Explor. 133, 25–41.
Shavers, E.J., Ghulam, A., Encarnacion, J., Bridges, D.L., Luetkemeyer, P.B., 2016. Carbonatite associated with ultramafic diatremes in the Avon Volcanic District, Missouri, USA: field, petrographic, and geochemical constraints. Lithos 248, 506–516.
Shavers, E.J., 2017. Geochemistry and Multiscale Remote Sensing of Carbonatite-ultramafic Intrusive Lithologies (Doctoral dissertation). ProQuest, pp. 11674.
Shavers, E.J., Ghulam, A., Encarnacion, J., Hartling, S., 2017. Emplacement of ultramafic-carbonatite intrusions along reactivated North American mid-continent rift structures. Tectonophysics 712–713, 716–722.
Środoń, J., Drits, V.A., McCarty, D.K., Hsieh, J.C.C., Eberl, D.D., 2001. Quantitative X-ray diffraction analysis of clay-bearing rocks from random preparations. Clays Clay Miner. 49 (6), 514–528.
Stagakis, S., Markos, N., Sykioti, O., Kyparissis, A., 2010. Monitoring canopy biophysical and biochemical parameters in ecosystem scale using satellite hyperspectral imagery: An application on a Phlomis fruticosa Mediterranean ecosystem using multiangular CHRIS/PROBA observations. Remote Sens. Environ. 114 (5), 977–994.
Walter, A.-V., Nahon, D., Flicoteaux, R., Girard, J., Melfi, A., 1995. Behaviour of major and trace elements and fractionation of REE under tropical weathering of a typical apatite-rich carbonatite from Brazil. Earth Planet. Sci. Lett. 136 (3), 591–602.
Woolley, A.R., Kjarsgaard, B.A., 2008. Carbonatite occurrences of the world: map and database, Geologic Survey of Canada.
Wyllie, P., Tuttle, O., 1960. The system CaO–CO2–H2O and the origin of carbonatites. J. Petrol. 1 (1), 1–46.
Xie, Y., Li, Y., Hou, Z., Cooke, D.R., Danyushevsky, L., Dominy, S.C., Shuping, Y., 2015. A model for carbonatite hosted REE mineralisation — the Mianning–Dechang REE belt, Western Sichuan Province, China. Ore Geol. Rev. 70, 595–612.